

# Red Clump Morphology as Evidence Against an Intervening Stellar Population as the Primary Source of Microlensing Toward the LMC

Jean-Philippe Beaulieu and Penny D. Sackett

Kapteyn Astronomical Institute 9700 AV Groningen, The Netherlands

beaulieu@astro.rug.nl,psackett@astro.rug.nl

## ABSTRACT

We examine the morphology of the color-magnitude diagram (CMD) for core helium-burning (red clump) stars to test the recent suggestion by Zaritsky & Lin (1997) that an extension of the red clump in the Large Magellanic Cloud (LMC) toward brighter magnitudes is due to an intervening population of stars that is responsible for a significant fraction of the observed microlensing toward the LMC. Using our own high resolution CCD photometry of several fields across the LMC, we confirm the presence of this additional red clump feature, but conclude that it is caused by stellar evolution rather than a foreground population. We do this by demonstrating that the feature (1) is present in all our LMC fields and in some fields extends to slightly fainter as well as brighter magnitudes compared to the primary clump, (2) is in precise agreement with the location of the blue loops in the isochrones of intermediate age red clump stars with the metallicity and age of the LMC, and (3) is present in the Hipparcos CMD for the solar neighborhood where an intervening population cannot be invoked. Finally, we show that current understanding of stellar evolution and LMC star formation history is consistent with the features seen not only in our data, but also the LMC CMD of Zaritsky & Lin.

*Subject headings:* Galaxies: Individual (LMC, Sgr) — Galaxies: kinematics and dynamics — Galaxy: halo — Local Group — dark matter Stars: intermediate age

## 1. Introduction

The recent discovery of an overdensity of stars in the color-magnitude diagram (CMD) of the Large Magellanic Cloud (LMC) having nearly the same color as the “red clump” but extending to magnitudes  $\sim 0.9$  mag brighter has been interpreted as an intervening population of stars at  $33-35$  kpc that may represent tidal debris sheared from a small Milky Way satellite (Zaritsky & Lin 1997, hereafter ZL). Zaritsky & Lin label this overdensity the VRC (vertical extension of the red clump), and reject other possible explanations to conclude that the VRC represents a massive foreground population with about 5% of angular surface density of the LMC itself. If true, this conclusion would have profound consequences for the interpretation of Galactic microlensing studies (Renault et al. 1997, Alcock et al. 1997b) since such debris could, in principle, be responsible for a sizable fraction of the microlensing signal toward the LMC (Zhao 1996, 1997) that is generally attributed to microlensing by compact objects in the smoothly-distributed halo of the Milky Way itself.

The foreground interpretation has been challenged by the MACHO team, who find no evidence in their extensive photometric database for RR Lyrae or Cepheids associated with a foreground population at 34 kpc (Alcock et al. 1997a). They do find an overdensity of stars in a composite MACHO  $R$  versus  $V - R$  color-magnitude diagram (CMD), but conclude that the *redder* color of this supra-clump is incompatible with the hypothesis of a foreground population. (We will show that the supra-clump found by MACHO is unlikely to be the VRC, but rather the red giant branch bump (RGBB), another phase of stellar evolution.) Gould (1997) argues on the basis of surface photometry of LMC performed by deVaucouleurs (1957) that one of the following is true about the foreground population: (1) it does not extend more than  $5^\circ$  from the LMC center, (2) is smooth on  $15^\circ$  scales, (3) has a stellar mass-to-light ratio 10 times that of known populations, or (4) provides only a small fraction of the microlensing optical depth. Using a semi-analytic method to determine the phase space distribution of tidal debris, Johnston (1997) has analyzed the Zhao (1997) proposition concluding that an ad hoc tidal streamer to explain the microlensing optical depth toward the LMC would cause unobserved overdensities of 10-100% in star counts elsewhere in the Magellanic Plane or would require disruption precisely aligned with the LMC within the last  $10^8$  years.

Using high resolution BVR CCD photometry of several fields at different locations in the LMC, we confirm the presence of substructure in LMC red clump morphology corresponding to the VRC observed by ZL. In contrast to ZL, however, we argue that the origin is likely to be due to stellar evolution, not an intervening population. We begin by illustrating that the VRC is seen in all our fields, but because the red clump morphology varies slightly in color and magnitude over the face of the LMC, interpretation of composite

CMDs is complicated by the superposition of different features. We therefore focus on one of our LMC fields, which exhibits a smooth nearly colorless feature that extends to magnitudes both fainter and brighter than the main clump, unlike what would be expected for a purely intervening population at  $33 - 35$  kpc. By overlaying our LMC color-magnitude diagrams with isochrones of the appropriate metallicity and age, we demonstrate that the VRC corresponds precisely in magnitude and color to the so-called “blue loops” experienced by aging intermediate-mass core He-burning stars. We then show that similar red clump morphology is present in the CMD of Hipparcos, which probes stellar populations on scales of 100 pc from the Sun, where intervening dwarf galaxies or tidal debris cannot be invoked. Finally, we analyze the argument used by ZL to reject stellar evolution as the cause of the VRC, and show that a more realistic model for the star formation history in the LMC is not only consistent with the VRC, but also provides a better fit to the data.

## 2. New BVR LMC Photometry

In January 1994, Bessel BVR photometry was performed with the Danish 1.5m telescope at ESO La Silla on the EROS#1, EROS#2 and MACHO#1 microlensing candidates; a fourth field was taken far from the bar; we will refer to these fields as F1, F2, F3 and F4 respectively. The detector was a thinned, back-illuminated, AR-coated Tektronix  $1024 \times 1024$  CCD with a nominal gain of 3.47 e-/ADU, readout noise of 5.25 e rms, and pixel size of  $24\mu\text{m}$  corresponding to  $0.38''$  on the sky. The detector is linear to better than 1% over the whole dynamic range and is not affected by any large cosmetic defects. Observational and field characteristics are listed in Table I. The CMD of these fields have been used to calibrate data obtained by the EROS microlensing survey, further details can be found in Beaulieu et al. (1995).

We have performed a reanalysis of these BVR data with DoPhot (Schechter, Mateo & Saha 1993). Typical DoPhot reported errors on relative photometry are 0.02 mag at  $V = 19$  (typical for the clump stars) for the cosmetically superior (DoPhot type 1) stars used throughout this analysis. Absolute calibration was performed using Graham (1982) and Vigneau & Azzopardi (1982). Foreground extinction was estimated using H I and IRAS maps (Schwering & Israel 1991); these corrections are listed in Table I for every field. Beginning with this foreground extinction and assuming a metallicity of  $Z = 0.008$  for the LMC and a helium abundance of  $Y = 0.25$ , we then vary the internal extinction to achieve the best fit of the main sequence to the isochrones of Bertelli et al. (1994). In fields F1 and F4, this produces a total extinction equal to that of the foreground (no internal reddening); in fields F2 and F3, the internal extinction results in an additional  $E(B - V)_{\text{int}} = 0.04$ . We

will show that although correcting for extinction is important, the difference between the foreground reddening and the reddening determined from main sequence fitting does not affect our conclusions.

## 2.1. Features in the New LMC Color-Magnitude Diagrams

A calibrated composite  $(V - R) - V$  CMD for all four fields is shown in Fig. 1 both with and without extinction corrections for the individual fields. First identified by Cannon (1970), red clump stars are the counterpart of the older horizontal branch (HB) in globulars, and represent a post helium-flash stage of stellar evolution (for a review, see Chiosi, Bertelli & Bressan 1992). The clump is clearly visible in the composite CMD at about  $V_0 \approx 18.7$  and  $(V - R)_0 \approx 0.5$  ( $(B - V)_0 \approx 0.9$ ). A narrow vertical extension of the clump having nearly the same color as the peak red clump density but extending up to  $\sim 0.8$ mag brighter can also be seen. Although confusion with the red giant branch makes delineating the fainter regions of this extension difficult, contour plots of CMD of Field F2 (which suffers the least crowding) indicate that this vertical feature extends below the peak red clump density to somewhat fainter magnitudes as well. A second source of substructure, or “supra-clump,” is apparent at a position  $\sim 0.8$  mag brighter in  $V$ , and  $\sim 0.1$ mag redder in  $(V - R)$  than the peak of the primary red clump. The positions of these features are marked in Fig. 1.

This substructure can be seen not only in the composite CMD, but also in the calibrated, extinction-corrected  $(V - R) - V$  CMDs for each of the individual new four LMC fields presented in Fig. 2. Fields F1 and F3 are located close to the LMC bar; fields F2 and F4 further away at about  $2 - 3^\circ$  from the center of the LMC. The magnitude and direction of the reddening vector is shown for each field. Comparable CMD have been presented and analyzed by Vallenari et al. (1996, and references therein). Our analysis is aimed at an understanding of the nature of the morphology of the red clump region in order to test the hypothesis that the VRC is due to an intervening stellar population.

Examination of Fig. 2 indicates that although the overall morphology of the CMD is the same in each field, the extent of the red clump and stellar density along the main sequence varies from field to field. This complicates any analysis that rests on a composite CMD drawn from several regions of the LMC. We also caution that comparisons between the stellar density in the red clump and main sequence regions of the CMD must be done with extreme care due to the selection effects induced by crowding. Less severe crowding has clearly resulted in deeper photometry for the F2 field, for example, and thus a larger number of main sequence stars. Selection effects due to differences in crowding will not play a strong role, however, in making comparisons between the stellar density in the VRC and

the red clump itself, since we expect to be complete at these magnitudes.

Since our four fields show indications of different star formation histories, we study them separately. Using contour plots of our four CMD, we determine the position of the red clump (at peak density) and the extent of other substructures relative to the primary clump. The results are summarized in Table II. The *relative* position of the vertical extension is remarkably constant in each of our fields and is also consistent with that found by ZL: we find that the vertical extension has a  $V - R$  color that varies no more than 0.03 mag from that of the primary clump peak and that it extends at least 0.8 mag brighter in  $V$  than the red clump peak. The second, redder substructure also maintains a constant relative position to the red clump from field to field. To within 0.02 mag in every field, this supra-clump is 0.8 mag brighter in  $V$  and 0.10 mag redder in  $V - R$  than the peak density of the red clump.

Since the characteristics that we find in the two substructures, the vertical extension and the redder secondary peak are identical within the uncertainties to those found by ZL and the MACHO team respectively, we identify the vertical feature seen in our data with that discussed by ZL and the second redder feature with the additional clump discussed by Alcock et al. in what follows. In the following section we propose stellar evolutionary origins for each of these features.

## 2.2. Analysis of the Individual CMDs

The position of red clump stars on a color-magnitude diagram depends on their mass, and thus on their age as they pass through this evolutionary stage. Using the isochrones of Bertelli et al. (1994), we plot in Fig. 3 the mean locus of the core Helium-burning phase with their ages labeled in a  $(B - V) - V$  CMD. We have used tracks with metallicity and helium abundance appropriate to the LMC, namely  $Z = 0.008$  and  $Y = 0.25$ . Note that clump stars with ages in the range  $\log(\text{Age}) = 8.6 - 9$  exhibit color changes smaller than 0.03 mag in  $(B - V)$  while differing in  $V$  magnitude by 0.79 mag. We now compare these theoretical expectations with our own LMC data.

To avoid the difficulties arising from composite CMDs, we begin by focusing on field F2 for which we have obtained the best photometry due to the low level of crowding in this outer field. The luminosity function in this field is still rising at a magnitude of  $V = 22$ . In the upper panel of Fig. 4, the  $(B - V) - V$  CMD for field F2, dereddened by  $E(B - V) = 0.12$ , is shown. We have overplotted theoretical isochrones (Bertelli et al. 1994) computed with new radiative opacities (OPAL) for  $Z = 0.008$  and  $Y = 0.25$ ,

appropriate to the LMC. Isochrones with ages corresponding to 0.25, 0.40, 0.63, 1.0 and 2.5 Gyr ( $\log(\text{Age}) = 8.4, 8.6, 8.8, 9.0$  and  $9.4$ ) are shown. The lower panel enlarges the region of the CMD near the red clump region, which is now plotted as contours under the mean locus of the core He-burning phase from Fig. 3.

The same 2.5 Gyr isochrone from Bertelli et al. (1994) was used by ZL as the best fit to the red clump morphology seen in their LMC data. If, following ZL, we do not apply an extinction correction, the 2.5 Gyr does indeed provide a plausible fit to the red giant branch. With our extinction correction, however, this isochrone falls at the very reddest (or oldest) edge of the red clump in field F2, as can be seen in Fig. 4. As Fig. 5 illustrates, this is true for all of our fields. Note that if we had applied only foreground extinction corrections due to the Milky Way itself, the discrepancy with the 2.5 Gyr isochrone would still be present: for two fields the internal extinction (as determined by our main sequence fitting) is negligible, for two others  $E(B - V)$  is increased by only 25 - 33%. Furthermore, younger isochrones fit the red clump of each field similarly despite the fact that different external extinction corrections (based on estimates from HI and IRAS data) were made. We take this as an indication that these extinction corrections are reasonable and necessary for the proper interpretation of the stellar evolution.

Fig. 5 shows that all our fields contain stars on the main sequence at least as young as 400 Myr. Field F3 in particular, which is closer to the bar, shows evidence both along the main sequence and in the region of the AGB that stars younger than 250 Myr are present. The more central fields also show slightly higher total extinction, and differential reddening may be responsible for the elongated, tilted bulge. It is likely that differences in the age distribution also play a role. Our outer fields show a clear deficit of stars of ages 1-3 Gyr compared to the fields closer to the bar, indicating that a recent burst of star formation following a period of quiescence. Such bursts of star formation as recent as a few 100 Myr ago have already been suggested for the LMC (e.g., Bertelli et al. 1994, Girardi et al. 1995).

Close examination of the CMD of field F2 in Fig. 4 indicates that the VRC extends to fainter magnitudes as well, a characteristic that would not be expected for a purely foreground population. Such a feature is easily explained, however, by core He-burning stars of intermediate masses and ages between  $\sim 0.4$  and  $\sim 1.0$  Gyr. Stars of these masses experience the well-known “blue loops” (see e.g., Sweigart 1987, Chiosi et al. 1992) that are caused by the increasing temperature of the outward expanding H-burning shell as the He-burning core gains mass. When the hydrogen in the shell is exhausted and helium begins to burn in the shell, the star moves redward again in the CMD to quickly join the asymptotic giant branch (AGB). During this phase, stars spend most of their time near the bluest end of the blue loops, with the position of the most blueward extension for

stars in the mass range  $\sim 2 - 3M_{\odot}$  differing substantially in luminosity, but very little in color (Fagotto et al. 1994). Fig. 4 indicates that both the faint end of the VRC which extends below the peak clump luminosity and the brighter end can be explained by stars of ages  $\sim 0.4$  and  $\sim 1.0$  Gyr undergoing blue loops. The agreement is remarkable, especially considering that we have not adjusted the metallicity of the isochrones to achieve a better fit. That such young stars are present in the LMC is clearly demonstrated by the presence of stars on the upper main sequence corresponding to these ages. We therefore conclude that intermediate mass stars in the LMC currently undergoing core He-burning are responsible for the VRC.

Due to the centering of the supra-clump seen both in our data and in the composite CMD of the MACHO database (Alcock et al. 1997a) on the red giant branch, is likely that this second substructure is due to the so-called “red giant branch bump” (RGBB, see e.g., Rood 1972, Sweigart, Greggio & Renzini 1989, and Fusi Pecci et al. 1990). During evolution along the red giant branch, color and luminosity evolution pauses as the H-burning shell passes through a discontinuity left by the maximum penetration of the convective envelope. This results in an overdensity along the red giant branch. Using an LMC distance modulus of 18.5, the apparent magnitude of the RGBB (Sweigart, Greggio & Renzini 1989) for the LMC metallicity and helium abundance that we have assumed here agrees with the position and extent of the supra-clump in our data. Zaritsky & Lin (1997) have also made this identification in their own data. Both secondary features in the CMD are thus explained by stellar evolution: the VRC by young stars of intermediate-mass experiencing core He-burning and the RGBB by a slowing of evolution along the red giant branch for somewhat older H-burning stars.

### 2.3. Relative Stellar Densities in the Composite CMD

We now pose two questions: (1) Is the relative stellar density in our CMD within the region of the VRC consistent with that found by ZL? (2) Is this stellar density consistent with that expected from a simple model of star formation history and evolution?

To compare with ZL, we return to our composite, dereddened  $(V - R) - V$  CMD, using boxes in color-magnitude space to define the vertical extension ( $0.4 \leq (V - R) \leq 0.5$ ,  $17.7 \leq V \leq 18.3$ ), the supra-clump or RGBB ( $0.5 \leq (V - R) \leq 0.65$ ,  $17.7 \leq V \leq 18.3$ ) and primary clump ( $0.4 \leq (V - R) \leq 0.6$ ,  $18.4 \leq V \leq 19.5$ ). The counts within these regions of our composite CMD are 200, 351 and 2442 stars respectively, indicating that the VRC has a density  $\sim 8\%$  and the RGBB  $\sim 14\%$  that of the primary clump. Slightly different choices for the relevant boxes, for example narrowing them to reduce contamination from stars in

other stages of stellar evolution, yield very similar fractions. Since our VRC estimate has an uncertainty of  $\sim \pm 1\%$  from counting statistics alone, it is consistent with the Zaritsky & Lin estimate of  $\leq 7\%$  for the relative projected angular surface density of the VRC.

Detailed models for the stellar density in a particular region of the CMD must combine stellar evolution with assumptions about the star formation history and the initial mass function (IMF) of the population. In Fig. 6, we show the centroid of the core He-burning stars taken from the appropriate models of Bertelli et al. (1994) overplotted on contours of the stellar density for each of our fields separately. Each field shows evidence for a VRC corresponding with core He-burning stars with  $\log(\text{Age}) \sim 8.6$  (400 Myr), but fields F1 and F3 closer to the bar of the LMC show a higher stellar density in the regions of the CMD corresponding to clump stars with  $\log(\text{Age}) \sim 9.2$  (1.6 Gyr). We caution that the different star formation histories of our fields complicates detailed modeling of the stellar densities in the CMD, and proceed with only a simple order-of-magnitude estimate to determine whether simple assumptions can populate the VRC with the observed relative density.

We assume that star formation was active and constant at some arbitrary rate between epochs  $8.5 \leq \log(\text{Age}) \leq 9.2$  ( $0.3 \leq \text{Age} < 1.6$  Gyr) and that the initial mass function is given by a Salpeter law with  $dN = A M^{-2.35} dM$  (Salpeter 1955). Since we are interested in relative star counts, the normalization factor  $A$  is arbitrary and irrelevant. Using models of Bertelli et al. (1994) which predict the mean mass and age of core He-burning stars in a given portion of the CMD (Fig. 3), we can then count the stars within a given age (mass) ranges and compare their ratios with that expected for our simple star formation assumptions.

We consider two age ranges corresponding to He-burning stars in the upper VRC ( $0.35 - 0.45$  Gyrs) and lower VRC and primary clump ( $0.6 - 1.2$  Gyrs) over which star formation can reasonably be expected to have been constant in all our fields. Within these age ranges, core He-burning stars in the upper VRC are expected to have masses in the range  $\sim 2.8 - 3.1 M_{\odot}$ , while those in the lower VRC and primary clump have masses in the range  $\sim 1.9 - 2.5 M_{\odot}$ . IMF considerations alone would thus predict  $\sim 13$  times more stars in the main clump than in the VRC. (The masses quoted here are the masses during this phase of evolution; in this order-of-magnitude calculation we have not considered the relative differences in mass evolution since the main sequence turn-off.) Since stars in the lower mass range evolve over the tip of their blue loops about 3.5 times more slowly than stars in the higher mass range (Fagotto et al. 1994), the overall expectation is that the upper VRC should have a stellar density of  $\sim 2\%$  that of primary clump. Stars with masses of  $\sim 4 M_{\odot}$ , corresponding to ages of 200 Myr in the core He-burning phase evolve so quickly that they would not be expected to be detected in the clump region of the CMD. This may

explain the bright end cutoff of the VRC. The VRC fraction depends fairly sensitively on the star formation history — decreasing if there has been no star formation over the last 500 Myr and increasing if there has been a burst within the last 500 Myr. We note that Giraldi et al. (1995) have suggested a burst as recent as 100 Myr based on the integrated colors of LMC star clusters. Our rough prediction for the relative density of the VRC is within a factor of three of the 5 – 7% measured by ZL, and within a factor of four of our own measurement of  $\sim 8\%$ . Given the uncertainty in this simple model of star formation history, contamination in the CMD from stars at different stages of their evolution, and the possibility that the IMF for stars above  $2 - 3 M_{\odot}$  deviates somewhat from the Salpeter law (Vallenari 1996), this order of magnitude estimate from stellar evolution is consistent with observations.

### 3. The Red Clump Vertical Extension in the Hipparcos CMD

The parallaxes obtained by the Hipparcos mission have allowed the determination of distances to stars brighter  $M_V = 8$  with accuracies on the order of 10% (Perryman 1997). This has resulted in a more accurately-determined color-absolute magnitude diagram for stars within  $\sim 100$  pc than has heretofore been possible, resulting in the first clear detection of “clump giants” in the solar neighborhood (Perryman 1995). Paczyński & Stanek (1997) conclude from their analysis that the Hipparcos red clump has a mean distance of 105 pc and a geometrical mean distance of 98 pc, making it unlikely that extinction significantly affects the magnitude or color of the clump.

In Fig. 7, we show the color-absolute magnitude diagram for 16229 stars from the Hipparcos catalog with relative distances determined to within 10% and colors determined to within 2.5%. The main sequence is clearly seen; the widening at  $M_V \approx 6$  has been attributed primarily to dispersion in age and chemical composition, not to uncertainties in magnitude or distance (Perryman 1995 and references therein). The red clump is clearly visible as a highly concentrated collection of stars with a density peaking near  $V = 0.7$  and  $B - V = 1.0$ . The redward tail of the clump seen most clearly in the contours may be due to the red branch of the evolving core He-burning stars overlapping giant branch (i.e., pre-helium flash giants).

Also visible in the Hipparcos CMD is a vertical extension of the red clump toward brighter magnitudes; its color is indistinguishable from that of the peak of the red clump. Centered near  $V = -0.5$ , this feature which is clearly discernible by eye at  $0 < V < 1$  and  $0.9 < B - V < 1.1$ . Its presence and location is robust to a variety of different choices for the smoothing and contouring of the CMD. A second overdensity at somewhat fainter

magnitudes ( $0.5 < V < -0.75$ ) and redder colors ( $1.1 < B - V < 1.3$ ) is also apparent, and corresponds to the position of the RGBB for stars of solar metallicity.

The isochrones overplotted in the upper panel of Fig. 7 assume a solar metallicity of  $Z = 0.02$  for stars of ages 0.4, 1.0, 2.5, 6.3 and 10.0 Gyr. It thus appears that the solar neighborhood has undergone some star formation in the last 400 Myr, but that the bulk of the stars in the red clump in the solar neighborhood are older than those of the LMC. The horizontal extent of the Hipparcos red clump is due to older stars that begin burning He in their cores at fainter, redder positions in the CMD and experience less severe blue loops. In the lower panel of Fig. 7, the area around the clump is enlarged and the stellar density plotted as contours. The VRC in the solar neighborhood can clearly be seen. Both the isochrones overplotted in the upper panel of Fig. 7 and the theoretical locus of core He-burning stars (of appropriate metallicity) overplotted in the lower panel make it clear that the VRC seen in the Hipparcos data is due to younger clump stars with ages between 300 Myr and 1 Gyr.

#### 4. The CMD Observations used by Zaritsky and Lin

The same vertical extension to the red clump is present in our LMC CMD and the CMD of ZL, yet we reach different conclusions as to its origin despite using the same isochrones from Bertelli et al. (1994) with the same metallicity  $Z = 0.008$  and helium abundance  $Y = 0.25$ . Why do our conclusions differ? ZL choose an isochrone with an age of  $\log(\text{Age})=9.4$  as the best match to the red giant morphology of their un-dereddened CMD. They then note that although younger isochrones with  $\log(\text{Age})=8.6$  can reproduce the increased luminosity of 0.9 mag observed in the VRC, the evolutionary models of Bertelli et al. predict a difference in color of the mean locus of the core He-burning phase of  $\Delta(B - V) = 0.13$  mag,  $\Delta(B - I) = 0.23$  mag between these two isochrones. Since they observe a color difference  $\leq 0.07$  in  $B - I$  between the VRC and the centroid of the red clump, they dismiss stellar evolution as the origin of the VRC. They further note that the maximum change in luminosity predicted by Sweigart (1987) for stars evolving in the clump is 0.6 mag compared with the 0.9 mag that they observe in their CMD.

If the CMD are first dereddened before comparing to model isochrones, and a (very) slight difference in ages of LMC stars is allowed, one reaches a different conclusion. Fig. 3 shows how the mean  $V$  magnitude of core the He-burning clump varies as a function of its  $B - V$  color for stars of different ages using the models of Bertelli et al. (1994). Indeed, as noted by ZL, a measurable color difference is expected between stars of  $\log(\text{Age})=8.6$  and  $\log(\text{Age})=9.4$ . However, as demonstrated by our Figs. 4 and 5, stars as old as 2.5

Gyr ( $\log(\text{Age})=9.4$ ) do not fit the dereddened red clump at all, and for some of our fields appear to be too red to fit the red giant branch as well. Dereddening by even 0.12 mag (comparable to the average *foreground* reddening of our LMC fields) has a dramatic effect on the conclusions since this shifts the mean age of the clump to younger ages for which the luminosity of the blue loops is a very strong function of age, while the color does not change appreciably. Thus, allowing for a very small range in the ages of young stars in the red clump is sufficient to reproduce the vertical extent of the VRC without significantly modifying its color. Note that this color insensitivity of the blue loops to age for stars between about 400 Myr and 1 Gyr is also true for the color defined by ZL ( $C \equiv 0.565 * (B - I) + 0.825 * (U - V + 1.15)$ ), as shown in Fig. 8 for regions of the CMD comparable to that shown by ZL in their Fig. 1.

We caution that studies made by Vallenari et al. (1996) and Bertelli et al. (1994) show that the star formation history in the LMC is variable from field to field and cannot be considered as a single burst of star formation 2.5 Gyrs ago. For example, in the outer region of the LMC (fields near NGC 1783, NGC 1866, NGC 2155), an intense burst episode began 3 – 4 Gyrs ago, and was sustained until a few 100 Myr ago. In other fields, an enhancement of star formation as old as 6 – 8 Gyrs is suggested by the data in the east of the bar (see Olszewski, Suntzeff & Mateo 1996 for a review of the old population). On the other hand, a burst at 1-2 Gyr followed by a period of quiescence and another burst at 100 Myr has been suggested by Girardi et al. (1995) on the basis of integrated colors of LMC star clusters. This variation in star formation history causes further difficulties for conclusions resting on composite CMD drawn from many fields or those that assume a single age for LMC stars.

Zaritsky & Lin note that if the foreground population hypothesis is correct for the origin of the VRC, then the entire LMC CMD should show traces of a parallel CMD shifted by 0.9 mag. They can find no such traces in their own data, but do point to the HST color-magnitude diagram of Holtzman et al. (1997) as corroborating evidence that such a parallel feature may be present in the lower main sequence of the LMC. They rightly note that binary stars would be a natural explanation for this excess of stars displaced by about -0.8 mag from the primary main sequence, but dismiss such an explanation as unappealing since it cannot simultaneously explain the VRC, for which they conclude that fine-tuning is required to ensure that both members of the binary arrive in this region of the CMD at the same time. ZL conclude that if binaries are invoked as an explanation for the excess population in the lower main sequence, another explanation is necessary for the VRC. While we make no claims as to the origin of a parallel main sequence in the LMC, we do proffer stellar evolution as the required alternate explanation for the VRC.

## 5. Conclusions

Using BVR color magnitude diagrams obtained in four different regions in the LMC, we confirm the presence of a vertical extension of the red clump having the same color as the clump peak, but extending to brighter magnitudes, as first mentioned by Zaritsky & Lin (1997). Unlike ZL, however, we conclude that this feature is due to stellar evolution, not a foreground population. Our argument is based on noting that the feature (1) extends to somewhat fainter as well as brighter magnitudes in some fields, (2) corresponds precisely to the location of the blue loops representing a relatively long-lived phase in the stellar evolution of younger core He-burning stars in the clump, and (3) is present in the solar neighborhood as demonstrated by the Hipparcos color-magnitude diagram.

The difference in our conclusions despite using the same model isochrones (Bertelli et al. 1994) rests on differences in our reddening corrections and assumptions about the ages of LMC stars. ZL perform no reddening correction, whereas we correct for reddening using main sequence fitting. This results in an average inferred  $E(B - V) = 0.14$ , only 0.02 mag greater than the average deduced for foreground extinction alone. ZL consider a single age of 2.5 Gyr for the clump with one possible burst at 400 Myr; whereas we consider a population more distributed in age and weighted toward younger ages than ZL. An isochrone of 2.5 Gyr does not provide a good fit to the red clump in any of our fields, whereas the presence of younger stars in all our LMC fields is clearly demonstrated by comparison of isochrones with the position of the clump and the upper main sequence. Stars of ages 0.4 – 1.0 Gyr are responsible for the full extent of the VRC, including stars both brighter and fainter than the peak of the primary clump.

With our assumptions, current understanding of stellar evolution predicts with remarkable precision the position of the VRC seen in both our data and the data of ZL, as well as a similar feature seen in the solar neighborhood. An order-of-magnitude calculation based on stellar evolution models combined with a simple model for the star formation history in these fields predicts the observed relative stellar densities in the vertical extension of the clump to within a factor of 3 – 4. We therefore conclude that no foreground population need be invoked to explain the presence of the VRC. Whatever the source of the microlensing optical depth toward the LMC, it is unlikely to be due to a foreground population that has made its presence evident in this vertical extension of the red clump.

We thank Konrad Kuijken useful discussion and for a prompt yet careful reading of the manuscript. We also thank E. Maurice and L. Prévot for advice on calibration procedures and R. Naber for with DoPhot subtleties. This work is based on observations carried out at the European Southern Observatory at La Silla.

## REFERENCES

Alcock et al. (The MACHO Collaboration) 1997, preprint, astro-ph/9707310

Alcock et al. (The MACHO Collaboration) 1997, *ApJ*, 486, 697

Beaulieu J.P. et al. (The EROS Collaboration) 1995, *A&A*, 299, 168

Bertelli, G., Bressan, A., Chiosi, C., Fagotto, F. & Nasi, E. 1994, *A&AS*, 106, 275

Cannon, R. D. 1970, *MNRAS*, 150, 111

Chiosi, C., Bertelli, G. & Bressan, A. 1992, *ARA&A*, 30, 235

de Vaucouleurs, G. 1957, *AJ*, 62, 69

Fusi Pecci, F., Ferraro, F.R., Crocker, D.A., Rood, R.T. & Buonanno, R. 1990, *A&A*, 238, 95

Girardi, L., Chiosi, C., Bertelli, G. & Bressan, A. 1995, *A&A*, 298, 87

Fagotto, F., Bressan, A., Bertelli, G. & Chiosi, C. 1994, *A&AS*, 105, 29

Gould, A. 1997, preprint, astro-ph/9709263

Graham J.A. 1982, *PASP*, 94, 244

Holtzman, J. et al. 1997, *AJ*, 113, 656

Johnston, K.V. 1997, preprint, astro-ph/9710007

King, C.R., Da Costa, G.S. & Demarque, P. 1985, *ApJ*, 299, 674

Olszewski, E.W., Suntzeff, N.B. & Mateo, M. 1996, *ARA&A*, 24, 511

Paczyński, B. & Stanek, K.Z. 1997 preprint, astro-ph/9708080

Perryman et al. 1995, *A&A*, 304, 69

Perryman et al. 1997, *A&A*, 323, L49

Renault C. et al. (The EROS Collaboration) 1997, *A&A*, 324, L69

Rood, R.T. 1972 *ApJ*, 177, 681

Salpeter, E.E. 1955, *ApJ*, 121, 161

Schechter P., Mateo M. & Saha A, 1993, PASP, 105, 1342

Schwering, P.B.W. & Israel, F. 1991, *å*, 246, 231

Seidel, E., Demarque, P. & Weinberg, D. 1987, ApJS, 63, 917

Sweigart, A.V., Greggio, L. & Renzini, A. 1989, ApJS, 69, 911

Sweigart, A.V. 1987, ApJS, 65, 95

Vallenari A., et al. 1996, A&A, 309, 367

Vigneau J., & Azzopardi M. 1982, A&AS, 50, 119

Zaritsky, D. & Lin, D.N.C. 1997 preprint, astro-ph/9709055 (ZL)

Zhao, H.-S. 1996 preprint, astro-ph/9606166

Zhao, H.-S. 1997 preprint, astro-ph/9703097

### Figure Captions

Fig. 1 — Calibrated, composite  $(V - R) - V$  color-magnitude diagrams for all four LMC fields described in the text. Only the 16,139 stars with cosmically superior point spread functions (DoPhot type 1) in  $V$  and  $R$  are plotted. Both uncorrected (left) and dereddened (right) CMD are shown. Positions of the red clump (RC), vertical extension to the red clump (VRC), and supra-clump or red giant branch bump (RGBB) are also indicated.

Fig. 2 — Calibrated, dereddened  $(V - R) - V$  color-magnitude diagrams for the individual four LMC fields. Only stars with cosmically superior point spread functions (DoPhot type 1) in  $V$  and  $R$  are plotted. The number of stars plotted is 3614, 4241, 5591, 2693 in  $V - R$  for fields F1 through F4 respectively.

Fig. 3 — Centroid of the  $V$ -band luminosity of the core He-burning phase as a function of  $B - V$  color for stars of different ages for  $Z=0.008$  and  $Y = 0.25$  (Bertelli et al. 1994). Note that no significant color change occurs for stars with ages between 400 Myr and 1 Gyr; these stars correspond to the VRC in the LMC. A similar sequence is for  $Z=0.02$  and  $Y=0.28$  (appropriate to the solar neighborhood), yields  $B - V$  color redder by  $\sim 0.1$ mag and is shown in Fig. 7. In the solar neighborhood, older stars are also present, causing the horizontal dispersion in color on the fainter edge of the red clump in the Hipparcos data.

Fig. 4 — **Top panel:** Calibrated, dereddened  $(B - V) - V$  color-magnitude diagram for our least crowded field F2. 4666 stars with cosmically superior point spread functions (DoPhot type 1) in  $B$  and  $V$  are shown. Isochrones with LMC metallicity ( $Z = 0.008$ ) and  $Y = 0.25$  with ages  $\log_{10}(\text{Age}) = 8.4, 8.6, 8.8, 9.0$ , and  $9.4$  from Bertelli et al. (1994) are shown superposed. **Bottom panel:** Contour representation of the CMD density for field F2 in region of the red clump shown superposed on the mean locus of the core Helium burning phase as a function of age as in Fig. 3. Separate scales for the abscissa of the top and bottom panels are indicated. The region of CMD shown has been divided into 25 bins along both the magnitude and color axes. For this binning, contour levels displayed are 12, 10, 8, 6, 4 and 2.5 stars.

Fig. 5 — Calibrated, dereddened  $(V - R) - V$  color-magnitude diagrams for each field as in Fig 2 with the isochrones from Fig. 4 overplotted.

Fig. 6 — Same as the bottom panel of Fig 4, but for all of our LMC fields. The region of CMD shown has been divided into 25 bins along both the magnitude and color axes. For this binning, contour levels displayed are 25, 20, 15, 12, 10, 8, 6, 4 and 2.5 stars. The highest contour levels are not always present in the outer fields.

Fig. 7 — **Top panel:** Hipparcos  $(B - V) - V$  color-magnitude diagram containing over 16000 stars with accurate distances and photometry. A vertical extension on the blueward side of the red clump with nearly the same color as the peak clump density and extending about a magnitude brighter can clearly be seen. The redder red giant branch bump (RGBB) is also visible. Isochrones with solar metallicity ( $Z = 0.02$ ) and  $\log_{10}(\text{Age})$  8.6, 9.0, 9.4, 9.8 and 10.0 are shown overplotted. Note that positions of the blue loops again coincide with the vertical extension. **Bottom panel:** Contour representation of the CMD density in region of the red clump for the solar neighborhood as measured by Hipparcos is shown superposed on the mean locus of the core He-burning phase as a function of age for stars with metallicity and helium abundance appropriate to the solar neighborhood ( $Z = 0.02$  and  $Y = 0.28$ ). Separate scales for the abscissa of the top and bottom panels are indicated. The region of CMD shown has been divided into 20 bins along both the magnitude and color axes. For this binning, contour levels displayed are 35, 25, 15, 10, 5 and 2.5 stars. The highest contour levels are not always present in the outer fields.

Fig. 8 — The same isochrones of LMC metallicity from Fig. 3 are plotted in color-magnitude diagrams for the region of the red clump. The color  $C \equiv 0.565*(B-I) + 0.825*(U-V+1.15)$  is that used by Zaritsky & Lin (1997) as are the bands on the vertical axis: U (top), B (middle), and I (bottom) respectively. Reddening vectors assuming an average  $E(B-V) = 0.12$  are shown in each panel. The blue loops correspond with the feature seen by ZL at a dereddened color of  $C \approx 2.9$ .

Table 1: Field center, seeing, and reddening determined from foreground and main-sequence fitting for each field.

Field	RA (J2000)	Dec (J2000)	Seeing	$E(B-V)_f$	$E(B-V)_{ms}$
F1	5h 26' 34"	−70° 57' 45"	1.0"	0.18	0.18
F2	5h 06' 05"	−65° 58' 03"	1.3"	0.08	0.12
F3	5h 14' 44"	−68° 48' 00"	1.0"	0.12	0.16
F4	5h 23' 00"	−66° 58' 00"	1.3"	0.12	0.12

Table 2: Position of the clump, relative limits of its vertical extension (VRC), and relative position of the supra clump or red giant branch bump (RGBB).

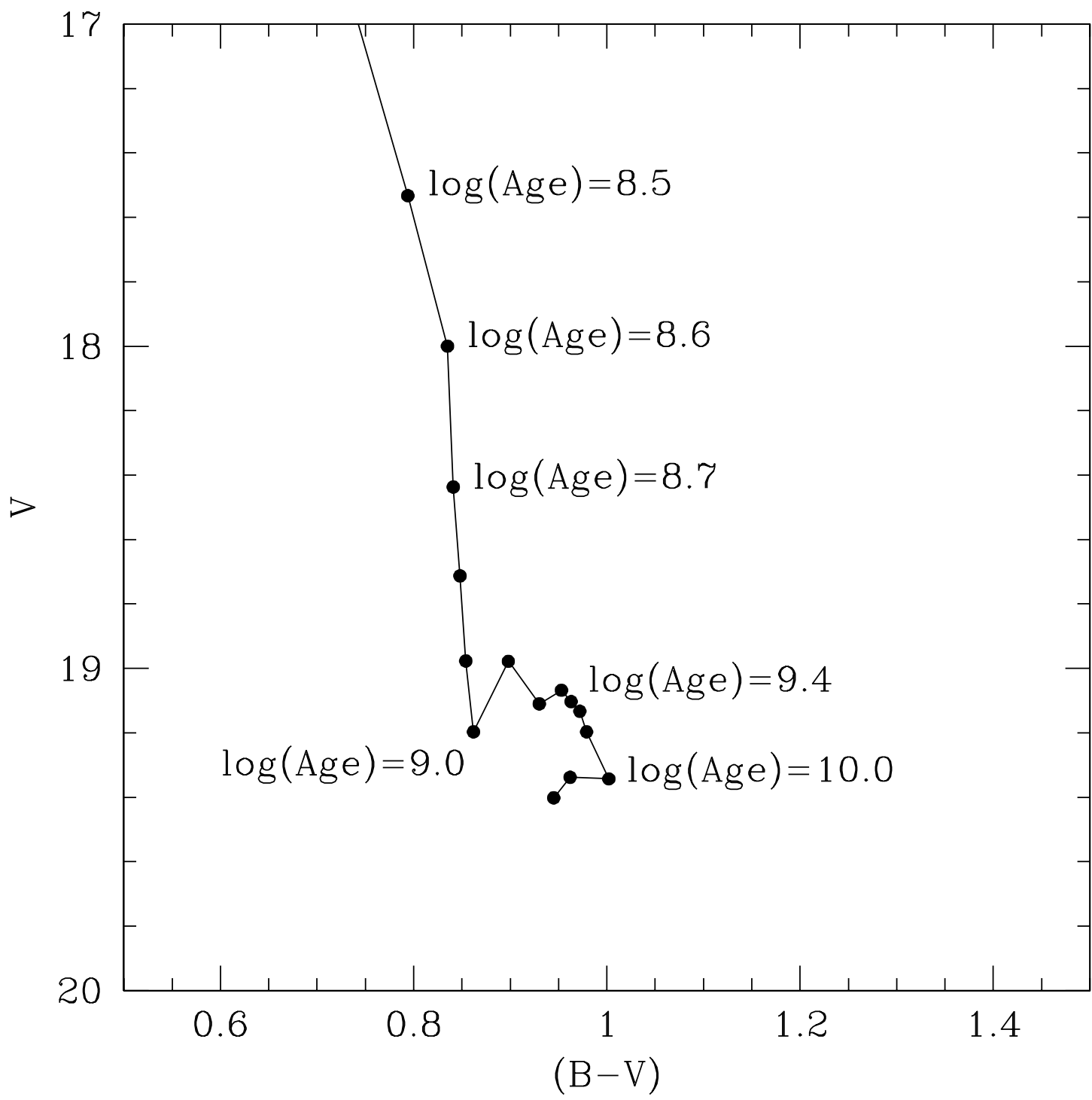
	F1	F2	F3	F4
Red Clump				
$V_0$	$18.67 \pm 0.03$	$18.65 \pm 0.02$	$18.68 \pm 0.03$	$18.70 \pm 0.02$
$(B - V)_0$	$0.87 \pm 0.01$	$0.86 \pm 0.01$	$0.85 \pm 0.01$	$0.88 \pm 0.02$
$(V - R)_0$	$0.48 \pm 0.01$	$0.48 \pm 0.01$	$0.48 \pm 0.01$	$0.48 \pm 0.01$
VRC				
$\delta V_0$	$-0.80 \pm 0.05$	$-0.82 \pm 0.05$	$-1.02 \pm 0.05$	$-0.63 \pm 0.1$
$\delta(B - V)_0$	$-0.01 \pm 0.01$	$0.01 \pm 0.01$	$0.01 \pm 0.01$	$0.00 \pm 0.02$
$\delta(V - R)_0$	$0.00 \pm 0.01$	$-0.02 \pm 0.01$	$0.00 \pm 0.01$	$0.00 \pm 0.02$
Supra Clump (RGBB)				
$\delta V_0$	$-0.82 \pm 0.05$	$-0.85 \pm 0.05$	$-0.84 \pm 0.05$	$-0.86 \pm 0.05$
$\delta(B - V)_0$	$0.24 \pm 0.02$	$0.24 \pm 0.02$	$0.20 \pm 0.02$	$0.25 \pm 0.02$
$\delta(V - R)_0$	$0.10 \pm 0.02$	$0.11 \pm 0.02$	$0.10 \pm 0.02$	$0.10 \pm 0.01$

This figure "beaulieusackett.fig1.gif" is available in "gif" format from:

<http://arxiv.org/ps/astro-ph/9710156v1>

This figure "beaulieusackett.fig2.gif" is available in "gif" format from:

<http://arxiv.org/ps/astro-ph/9710156v1>

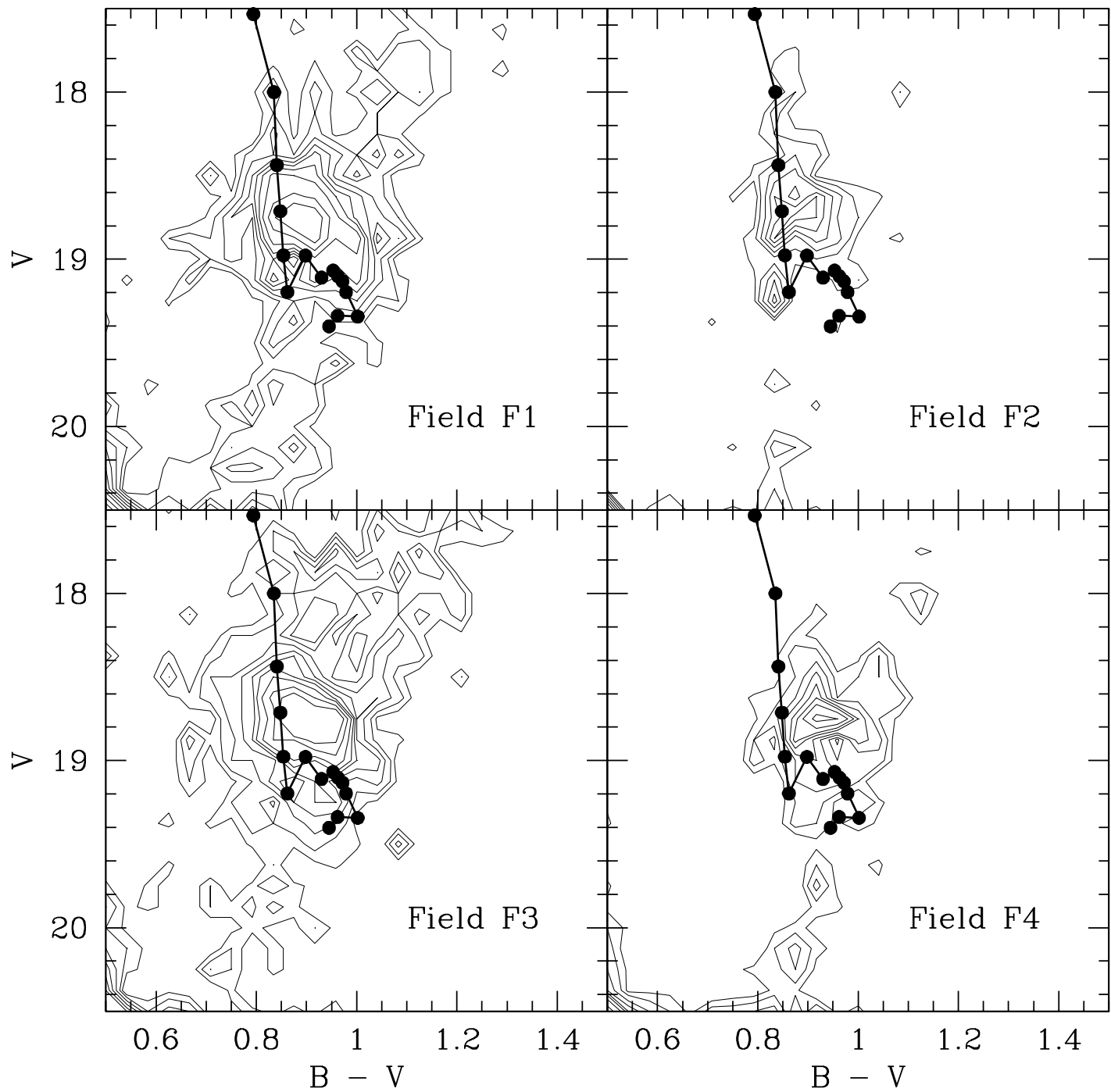


This figure "beaulieusackett.fig4.gif" is available in "gif" format from:

<http://arxiv.org/ps/astro-ph/9710156v1>

This figure "beaulieusackett.fig5.gif" is available in "gif" format from:

<http://arxiv.org/ps/astro-ph/9710156v1>



This figure "beaulieusackett.fig7.gif" is available in "gif" format from:

<http://arxiv.org/ps/astro-ph/9710156v1>

